Noninvasive vascular occlusion with HIFU for venous insufficiency treatment: preclinical feasibility experience in rabbits

N Barnat, A Grisey, B Lecuelle, J. Anquez, B Gerold, S. Yon, J.-F Aubry

Noninvasive vascular occlusion with HIFU for venous insufficiency treatment: preclinical feasibility experience in rabbits

AUTHORS/INSTITUTIONS:

N. Barnat[1, 2, 3, 4], A. Grisey[4], B. Lecuelle[5], J. Anquez[4], B. Gerold[4], S. Yon[4], J.-F. Aubry[1, 2, 3]

1- INSERM U979, Institut Langevin, Paris, France;

2- ESPCI Paris, PSL Research University, Institut Langevin, Paris, France;

3- CNRS UMR 7587, Institut Langevin, Paris, France;

4- Theraclion, Malakoff, France;

5- Ecole nationale vétérinaire d'Alfort, CRBM, Maisons-Alfort, France

Abstract

Venous insufficiency is a common disease arising when veins of the lower limb become incompetent. A conventional surgical strategy consists in stripping the incompetent veins. However, this treatment option is invasive and carries complication risks. In the present study, we propose noninvasive high-intensity focused ultrasound (HIFU) to treat lower limbs venous insufficiency, in particular incompetent perforating veins (mean diameter between 2-6 mm).

Sonication parameters were designed by numerical simulations using the k-Wave toolbox to ensure continuous coagulation of a vein with a diameter superior or equal to 2 mm. The selected ultrasound exposures were 4 seconds pulses in continuous wave mode. Two types of sonication were studied: (1) fixed pulses and (2) moving pulses at constant speed (0.75 $mm.s^{-1}$) across the vein.

The potential of these exposures to thermally occlude veins were investigated in vivo on rabbit saphenous veins. The impact of vein compression during ultrasonic exposure was also investigated.

Fifteen rabbits were used in these trials. A total of 27 saphenous veins (mean diameter 2.0 ± 0.6 mm) were sonicated with a transducer operated at 3 MHz. After a mean 15 days follow-

up, rabbits were euthanized and venous samples were extracted and sent for histologic assessment. Only samples with the vein within the HIFU lesion were considered for analysis. Simulated thermal damage distribution demonstrated that fixed pulses and moving pulses respectively placed every 1.5 and 0.5 mm along the vein and delivered at an acoustic power of 85 W and for 4 seconds were able to induce continuous thermal damages along the vein segments.

Experimentally, both treatment parameters (1) and (2) have proven effective to occlude veins with a success rate of 82%. Occlusion was always observed when compression was applied. Our results demonstrate that HIFU can durably and non-invasively occlude veins of diameters comparable to human veins.

Keywords: HIFU; ultrasound; thermal occlusion; vascular occlusion; vein

Introduction

Venous insufficiency is a common medical condition arising when a high pressure is transmitted from deep to superficial venous system of the lower limbs. High-pressure transmission frequently occurs through retrograde flow. This elevated venous pressure causes the vein to become tortuous and dilated over time. Besides the unsightly appearance of varicosities, venous disease is associated with pain and clinical signs may vary from asymptomatic telangiectasia to achy ulcer [1]. The strategy to treat venous disease consists in ceasing reflux by eliminating the involved incompetent vein segment.

Conventional surgical techniques consist in removing the vein. The invasive nature of surgery leads to the development of minimally invasive procedures such as radiofrequency ablation [2] or endovenous laser ablation [3]. In both cases, after introducing a catheter into the vein, thermal energy is delivered, in order to denature collagen and induce a shrinkage of the vein [4,5].

Although these techniques proved their efficacy, they are not appropriate to treat all leg veins. In case of incompetent perforating veins, thermal ablation is appropriate only for large (>3.5 mm) perforators and may treat perforators only superficially [6]. Furthermore, treating

pathologic veins can be technically challenging and requires experienced physicians especially for the insertion of the catheter in a deep or tortuous vein.

In this context, high-intensity focused ultrasound treatments (HIFU) could provide a non-invasive alternative to occlude incompetent veins.

Previous studies have demonstrated HIFU occlusion in blood vessels of small diameters only (range 0.5-1.5 mm) [7,8,17–21,9–16]. The occlusion of large vessels (≥2 mm) has not been reported to the best of our knowledge. We demonstrate here on a rabbit model that HIFU can occlude large veins (≥2mm), paving the way for a clinical treatment of venous insufficiency with focused ultrasound.

For this purpose, sonication strategies including placement and trajectory of pulses were first identified by numerical simulations and then evaluated on an *in vivo* model of rabbit veins (range: 1.1-3.7 mm).

Methods

Ultrasound equipment

Experiments were performed with the Echopulse® HIFU device (Theraclion, Malakoff, France) used clinically for human breast fibroadenomas [22] and benign thyroid nodules [23] treatments (Figure 1(a)). The system encompasses a treatment head mounted on an articulated arm which includes a single element piezocomposite therapy transducer and a linear confocal imaging probe for real-time monitoring of the treatment (Figure 1(b)). The therapy transducer, operated at 3 MHz, has a spherical cap shape with a curvature radius of 38 mm and an outer diameter of 56 mm. The RF signal applied to the transducer comes from a frequency generator (JJ&A Instruments, Model RFG-200T1) with an electric power ranging from 10 to 215 W. The ultrasound imaging probe working at a frequency of 6.2 MHz (Vermon, Tours, France) was connected to an Aixplorer® ultrasound system (SuperSonic Imagine, Aix-en-Provence, France) to guide treatments with B-mode images. By construction, the therapeutic focus is located within the imaging plane. A fluid-filled balloon

(EPack, Theraclion®, Malakoff, France) was fixed to the transducer to ensure acoustic coupling between the transducer and the target. The coupling liquid was circulated and cooled during all the procedure to avoid transducer overheating and skin burns. Cooling is ensured by built-in Peltier modules (Figure 1 (a)). A dedicated software implemented in MATLAB (MathWorks, Inc., Natick, Massachusetts, United States) was used to drive sonications.

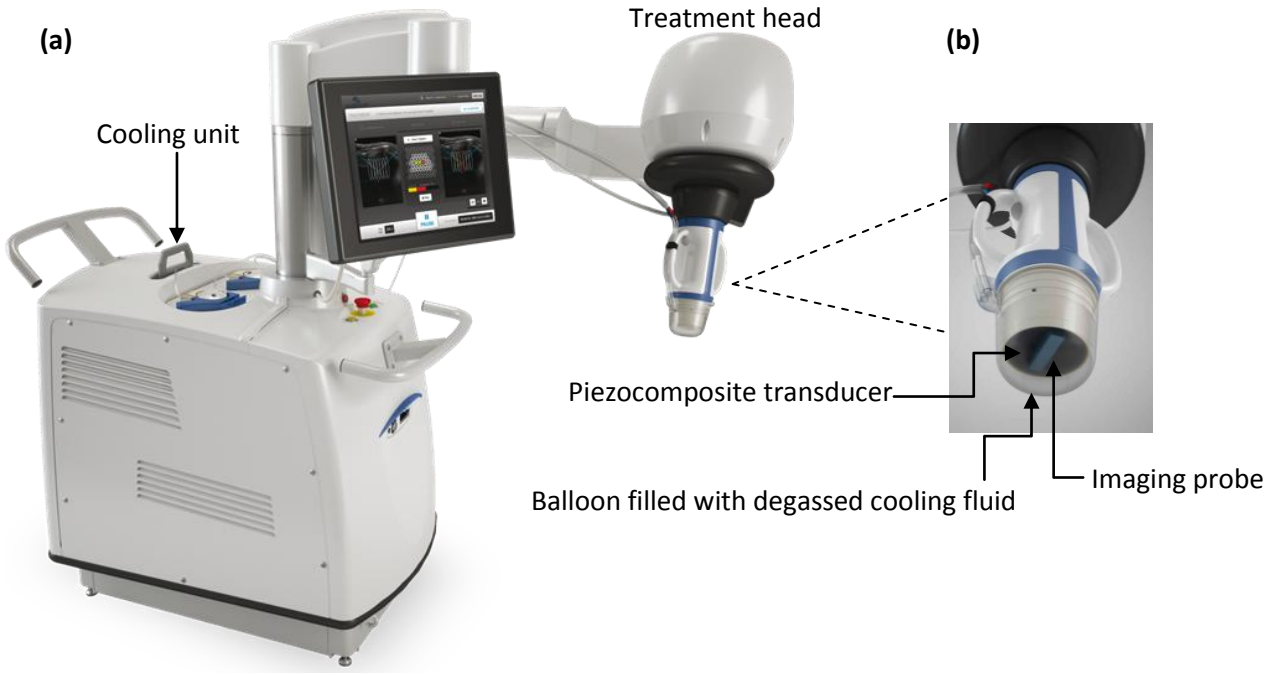

Figure 1: Ultrasound equipment: (a) Echopulse, (b) HIFU transducer.

Treatments simulation

Simulations were performed to adjust ultrasound exposures layout to adequately sonicate a vein of 2 cm in length and 2 mm in diameter. Two types of pulses were studied: (1) fixed pulses and (2) moving pulses at constant speed (0.75 $mm.s^{-1}$) along a line orthogonal to the longitudinal axis of the vein. In both cases, we used 4-second sonications delivered in continuous wave mode at an acoustic power of 85 W (typical power used in clinics and in our experiments) and with the focus located at 15 mm under the skin. Acoustic pressure field, temperature rise and, ultimately, thermal damages extent were simulated.

Geometrical model

The modelled HIFU transducer has the same geometry than the therapy transducer described in the Ultrasound equipment section. The frame of reference of the transducer was defined as follows: the origin corresponds to the HIFU transducer focus. X is the axis of the imaging transducer and oriented along the left-to-right direction of the generated images. Z denotes the main ultrasound propagation axis, pointing towards the subject anatomy. Y results from the cross product of Z and X, for the frame (X, Y, Z) to be orthonormal and right-handed.

In the simulations, the vein was considered as collapsed and the blood flow abolished. Thus, the vein itself was not modelled. We assumed that the ultrasound beam propagates through 3 layers, from top to bottom: (1) the cooling liquid contained in the balloon fixed to the transducer; (2) the skin and (3) the muscle. Skin was modelled as a 2-mm thick layer. For illustration purposes, a 2D view of the geometrical model is shown in Figure 2.

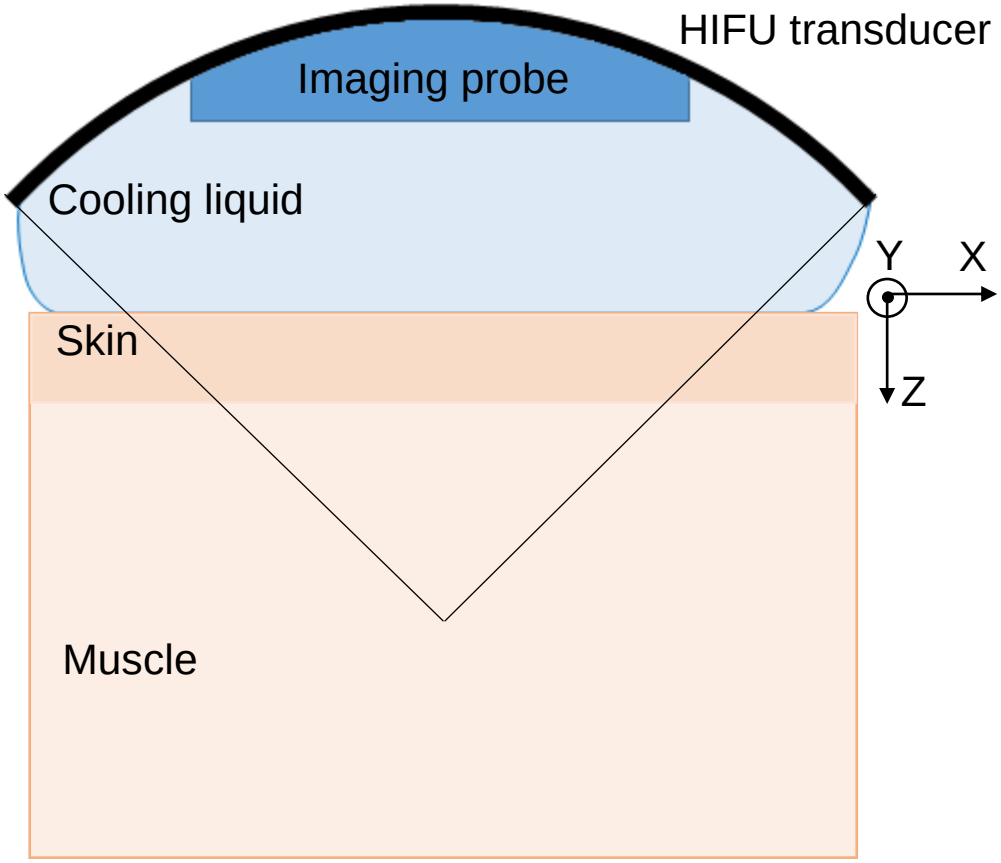

Figure 2: Model used in the simulations

Acoustic simulation

Acoustic simulations were performed using the k-Wave toolbox 1.2 [24]. The toolbox solves the system of coupled first-order partial differential equations comprising momentum conservation, mass conservation and pressure-density relation.

To solve the system of coupled acoustic equations, k-Wave uses a k-space pseudospectral method where spatial gradients are computed using the Fourier collocation spectral method [24]. Although the mathematical approach used in k-Wave is efficient, the 3D simulation of the HIFU beam is costly in terms of memory. In our case, at 3 MHz and considering a domain of $60\times60\times46$ mm, the simulation of the nonlinear propagation up to the fifth harmonic with the minimum of two points per wavelength requires a grid of 1.37×10^9 points. Hence, to reduce memory requirements, we used a "layer by layer" approach [25]. The computational grid is divided into finer and finer layers along the main propagation axis and we simulated ultrasound propagation from the transducer to 3 mm beyond the focus. We respectively used one layer for the cooling liquid, one layer for the skin and five layers for muscle tissue. Nonlinearities were modeled up to the fifth harmonic in the widest layer.

The size of the smallest layer was 4 x 4 x 4 mm (corresponding to 8 x 8 x 8 wavelengths), with a spatial grid step of 49.8 μm. A perfectly matched layer was used to avoid reflections at the boundaries of the domain.

The Courant-Friedrichs-Lewy (CFL) number was set to 0.5 resulting in a smallest time step of 14.8 ns. The pressure acoustic source term was computed as:

$$p^2 = \frac{2P_{ac}\rho c_s}{S_{transducer}}$$

The cooling liquid, skin, fat and muscle tissue were modeled as homogenous media with the acoustic properties listed in

Tissue properties were assumed to remain constant for the full procedure period. Variability of parameters with temperature was neglected for all simulations.

	Cooling liquid [26]	Superficial tissue (skin…)[26]	Muscle [27]
Sound speed ($m.s^{-1}$)	1495	1547	1587
Density ($kg.m^{-3}$)	1000	1214	1041
Attenuation at 3 MHz [$dB.cm^{-1}$]	0	2.2	3.0
Acoustic non-linearity parameter	4.9	9.0	7.8

Table 1: Acoustic properties of tissues used for simulations.

Thermal simulation

Tissue heating was modeled using the Pennes's bioheat equation [28]. The equation was solved in 3D using a first-order explicit Euler scheme in time and a centered scheme in space.

The time step was 50 ms and the spatial step was 200 μm. The grid size was 38 ×38×29 mm.

The heat source term was computed as stated in [25]. The classic attenuation model (absorption + scattering) was considered, and thermal rise was generated by the absorbing component.

The tissue initial temperature was set to $T_0 = 39.5$ °C which is the mean body temperature for a rabbit [29] and Dirichlet boundary conditions were used with $T_{boundaries} = T_0$. We modelled skin cooling as a heat flux at skin surface considering that the temperature of the cooling fluid was 10°C (value achieved during experiments) and the heat transfer coefficient between skin and liquid was set to 320 $W.m^2.K^{-1}$ based on previous experiments. To determine this value, temperature of skin was first measured several times with a thermocouple slipped between skin and the balloon in which circulated cooled liquid. Thereafter by assuming that heat flow at skin is proportional to the difference of temperatures between skin and a characteristic temperature of the cooling liquid, the value of 320 $W.m^2.K^{-1}$ has been assigned. As experimentally, the cooling time between subsequent sonications was set to 15 seconds.

The tissue properties used in thermal simulations are listed in Table 2 and were assumed invariant with temperature in simulations.

	Muscle[30]
Specific heat capacity ($J.kg^{-1}.K^{-1}$)	3600
Thermal conductivity ($W.m^{-1}.K^{-1}$)	0.47
Perfusion (s^{-1})	0.018

Table 2: thermal properties of media used in thermal simulation.

Thermal damage

To achieve vessel sealing, sufficient thermal damage shall be induced to the vessel wall. Modelling of vascular thermal damage [31] suggests that vessel thermal damage correlates with the denaturation of collagen fibrils, which begins at 62°C [32].

In this study, extent of thermal damage to vessels was evaluated based on a dedicated thermal damage model.

To assess the level of damage induced to vessels, we implemented the model described by Agah [31]. By considering denaturation of collagen as a first-order reaction, damage was modelled using a general Arrhenius equation:

$$\Omega(t) = \ln\left(\frac{c(0)}{c(\tau)}\right) = A_f \int_0^{\tau} \exp\left(\frac{-E_a}{RT(t)}\right) dt$$

Where:

Ω (t) is the damage parameter. $c(0)$, $c(\tau)$ are the concentrations of the undamaged molecules at the beginning and at time τ respectively. A_f is a coefficient of rate process (frequency factor), E_a the activation energy, R the universal gas constant, and T the temperature. A_f and E_a were set to $A_f = 5.6 \times 10^{63} s^{-1}$ and $E_a = 430$ kJ.mol^{-1} according to [31].

Degree of vessel damage is appraised by Ω (t), where $\Omega(t) = 1$ defines the first noticeable irreversible damage and formally corresponds to the denaturation of 63% of the native proteins [31]. As we are looking for an extensive damage to the vein, we set the threshold for thermal damage to $\Omega(t) = 5$, which formally corresponds to the denaturation of 99% of the collagen.

Animals

All animal work was approved by the institutional ethics committee for animal experiments (agreement number CE16/2016082512126208). Experiments were carried out according to the guidelines of the French National Comity for animal trials C.N.R.E.E.A (*Comité national de réflexion éthique sur l'expérimentation animale*). New-Zealand white rabbits (n=15), 5 males and 10 females, 2 to 4 months (3 ± 1) old and weighing 2.7 to 4.5 kg (3.5 ± 0.5), were used for the experiments. HIFU exposures were applied on medial saphenous veins. Prior to sonications, the animals were anesthetized intramuscularly with a mixture of Ketamine (0.33 mg/kg), Domitor (0.5 mg/kg) and Valium (0.17 mg/kg). They were then intubated with an endotracheal tube and ventilated with isoflurane to be kept under anesthesia throughout the procedure. The fur of their hind limbs was shaved with a hair trimmer and then carefully depilated with a depilatory cream to ensure good acoustic coupling and prevent skin burns.

HIFU procedure

Before the procedure, the rabbit was placed on the table in supine position to access the targeted vein. Ultrasonic gel (Polysonic Parker Laboratories, Inc., Fairfield, NJ) was applied to the area to be treated to ensure appropriate coupling. B-mode ultrasound and color Doppler imaging were used to position the focus on the vein.

27 medial saphenous veins (average diameter of 2 mm) were exposed to HIFU.

Blood flow is known to hamper thermal therapies by cooling down the vein wall [33–37]. Therefore, several configurations based on previous simulations were tested during the HIFU treatments: (1) 5 veins were treated with multiple pulses (median 1.5 mm spacing) distributed along the target vein (Figure 3A)); (2) 14 veins underwent the same treatment protocol than the one used in configuration (1) but the hind limb was elevated to about 25 degrees from the horizontal to diminish blood flow (Figure 3 B)); and (3) 8 veins were sonicated with moving pulses (0.75 $mm.s^{-1}$ along a 3-mm line transecting the vein) (**Erreur ! Source du renvoi introuvable.**) and were mechanically compressed by pressing a finger on the groin during exposures to stop blood flow and minimize its heat sink effect. Rear limbs elevation empty

veins of their intraluminal blood and induce venous spasm (illustrated in **Erreur ! Source du renvoi introuvable.** for configurations (2) and (3)). The average diameter of the vein after proximal compression was of 1 mm. According to simulations, for configuration 3, the spacing between moving pulses was reduced to 0.5 mm to account for the smaller lesion size in the longitudinal direction (Figure 3C)

Thus, the number of sonications was increased to sonicate the same length of 2 cm.

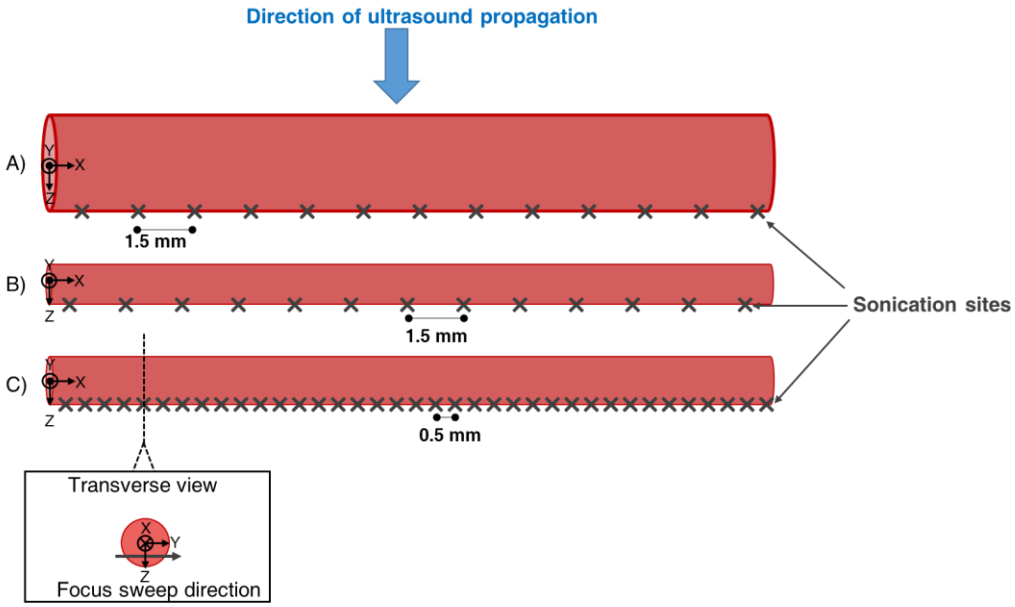

Figure 3: Schema illustrating dispositions of HIFU exposures. A), B) and C) stand for configurations (1), (2) and (3) respectively.

For all cases, HIFU sonications were applied for 4 seconds and at an acoustic power of 83 ± 10 W (obtained by multiplying electric power by the 70% efficiency of the transducer). The corresponding spatial-peak intensity (linear extrapolation from low power hydrophone measurement in water is 28 $kW.cm^{-2}$. A minimum time period of 15 s was set between two sonications to allow the skin to cool down. Experimental protocols are summarized in Table 3.

Experimental protocol ID	1	2	3
Number of HIFU exposed veins	5	14	8
Sonication types	Fixed pulses 1.5 mm apart	Fixed pulses 1.5 mm apart	Linear track with sites 0.5 mm apart Hind limb elevated

		Hind limb elevated	Vein compressed

Table 3: Experimental conditions

Histological protocol

After the experiments, the rabbits were recovered from anesthesia and were monitored for at least 15 days after treatment, to assess the sustainability of the effects of HIFU exposures on veins. Animals were then euthanized by intravenous injection of Pentobarbital (1 mL/kg).

The day of euthanasia, the animals underwent a *post mortem* dissection and the targeted vessel was harvested. In some cases, the perivenous conjunctive tissue was adherent and the vein could not be separated. In such cases, the vein was sent for analysis with the attached perivenous tissue.

The proximal tip of each venous section was sutured, preserved in identified cassettes, fixed in 4% formalin and sent for histologic examination. Samples were then cross-sectioned into 3 subsections and included in paraffin. 4-µm slices were cut and stained with haematoxylin-eosin (HE) for evaluation. Each section was evaluated without knowledge of the detailed treatment status.

Excision of the proper vein segment is difficult since other veins branch in the vicinity of the target. Therefore, samples were taken into account only when a vein was present on the slide and was located within the HIFU lesion.

A venous sample from untreated region was also extracted and served as a control.

Changes were graded as: normal vein (0), reactive endothelium (1), myoendothelial proliferation (2), acute fibrinous thrombi (3) and thrombus organization (4).

Results

Numerical model

Ultrasound pressure field

Figure 4 shows the rms acoustic pressure field profile in the YZ plane simulated with the "layer by layer" approach. Simulations were ran at 3 MHz and at an acoustic power of 85 W.

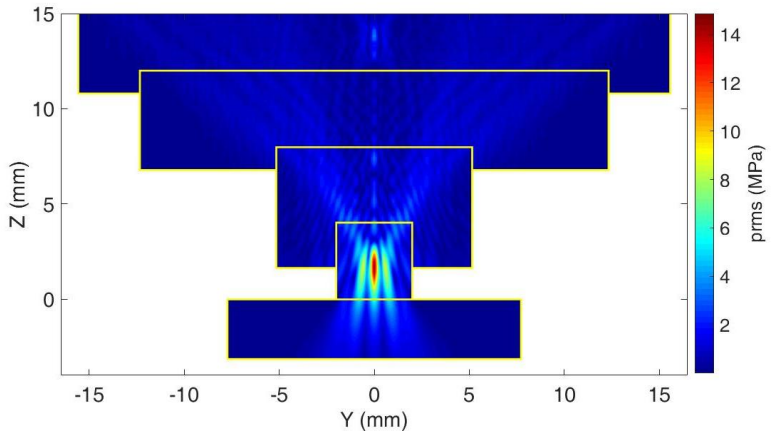

Figure 4: Simulated rms pressure field of the geometrical model in the YZ plane simulated. Pressure is expressed in MPa. Yellow rectangles represent the limits of the subsequent layers.

Thermal damages

Temperature elevation at the expected location of the upper vein wall (2 mm above the focal point centered on the lower vein wall) is plotted on Figure 5 for configurations (2) and (3).

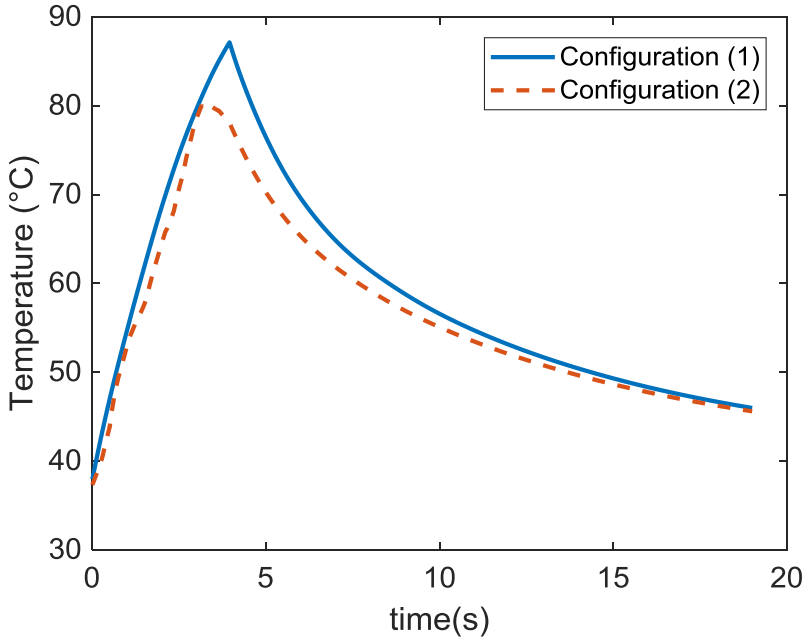

Figure 5: Simulated temperature elevation at the location of the vein wall during 4 s sonification followed by 15 s cooling for unitary fixed pulse (solid line) and moving pulse (dash line).

For unitary fixed and moving pulse, the extent of the coagulated zone as defined using the thermal damage model was 1.2 mm and 0.6 mm along the vein respectively and 1.8 mm and 2.7 mm in the orthogonal direction to the vein respectively.

To induce homogeneous and extensive heating of a vein 2 cm in length and 2 mm in diameter, we considered: (1) for fixed pulses, 13 sonications with a spacing of 1.5 mm and (2) for moving pulses, 37 sonications moving along the cross sectional axis with a spacing of 0.5 mm along the longitudinal axis of the vein.

Figure 6 and Figure 7 show the results of thermal damage distribution for such treatments: (1) 13 fixed pulses and (2) 37 moving pulses respectively. An iso-contour representing the area corresponding to denaturation of 99% of native proteins is displayed.

Distribution of thermal damage simulations are displayed using maximum intensity projections.

Figure 6: Maximum intensity projected damage map at the end of a treatment comprising thirteen 4-s fixed pulses delivered 1.5 mm apart at an acoustic power of 85 W and with the focus located at 15 mm under skin. Iso-contour corresponding to: the thermal damage where 99% of native proteins denature is displayed in black.

Figure 7: Projected damage map at the end of a treatment comprising 37 4-s pulses during which the focus was moved at 0.75 $mm.s^{-1}$. Sonications were delivered at an acoustic power of 85 W, with a spacing of 0.5 mm and with the focus located at 15 mm under skin. Iso-contour corresponding thermal damage where 99% of native proteins denature is displayed in black.

To quantify the impact of the trajectory, attention has been given to the extent of the region corresponding to protein denaturation.

Damaged zones in the XY plane of the vein for treatment layouts (1) and (2) are reported in Table 4.

Treatments ID	Damaged zone	Lesion area
(1)	19.2 × 2.4 mm²	42.8 mm²
(2)	19.2 × 4.2 mm²	72.0 mm²

Table 4: Simulated results in terms of damaged areas for treatment plannings (1) and (2)

After HIFU exposures, vessel damage can be observed through vessel shrinkage as illustrated in the following ultrasound image (Figure 8).

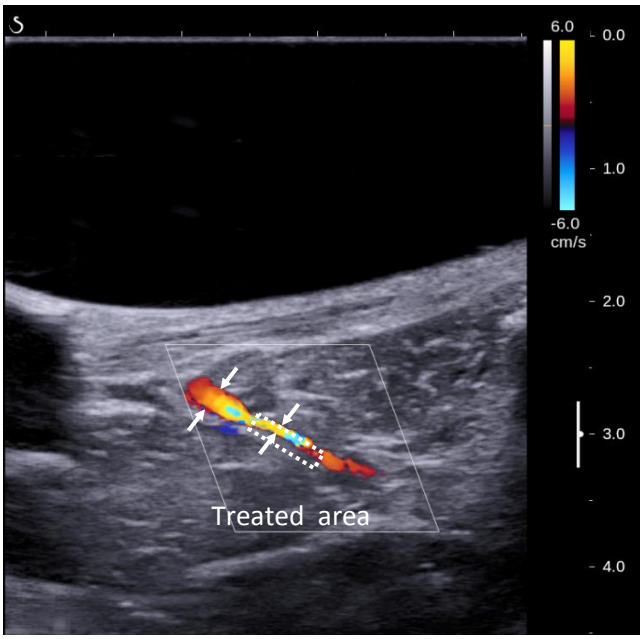

Figure 8: Acute vascular shrinkage following HIFU pulses

Histological findings

Clinical follow-up of the animals showed that recovery after HIFU treatments were well tolerated. All animals survived until the day of euthanasia and no abnormal behavior was noted postoperatively. All animals continued their normal pattern of feeding.

As mentioned in Histological protocol, only samples satisfying acceptance criterion were considered in the study.

In total and excluding the control sample, 17 samples (63%) were taken into account in this study. Histological results are reported in Table 5.

Experimental protocol ID	1	2	3
Number of accepted samples	1	10	6
Sonication types	Fixed pulses 1.5 mm apart	Fixed pulses 1.5 mm apart Hind limb elevated	Linear track with sites 0.5 mm apart Hind limb elevated Vein compressed
Follow-up duration	15 days	15 days	13 days
Occlusion score	**0**: 1/1	**0**: 2/10 **3**: 1/10 **4**: 7/10	**3**: 3/6 **3**: 3/6

Table 5: Results of vessel occlusion for each batch

The follow-up duration indicated in Table 5 corresponds to the median value. It is however necessary to emphasize that follow-up duration extended from 7 days for the shortest one to 19 days for the longest one due to the availability of the animal facility.

For all samples treated with fixed pulses and with a score superior or equal to 3, histological findings revealed a thrombo-vasculitis of the saphenous vein characterized by a transmural thickening and collapse of the lumen. Fibrinous thrombi were also present. These lesions are irreversible in nature or expected to be irreversible (as assessed by the histopathologist) for the samples with a follow-up duration inferior to 13 days. Lesions were expected to evolve towards the formation of large fibrotic scars incorporating saphenous veins. Figure 9 shows illustrative HE stained histologic cross sections.

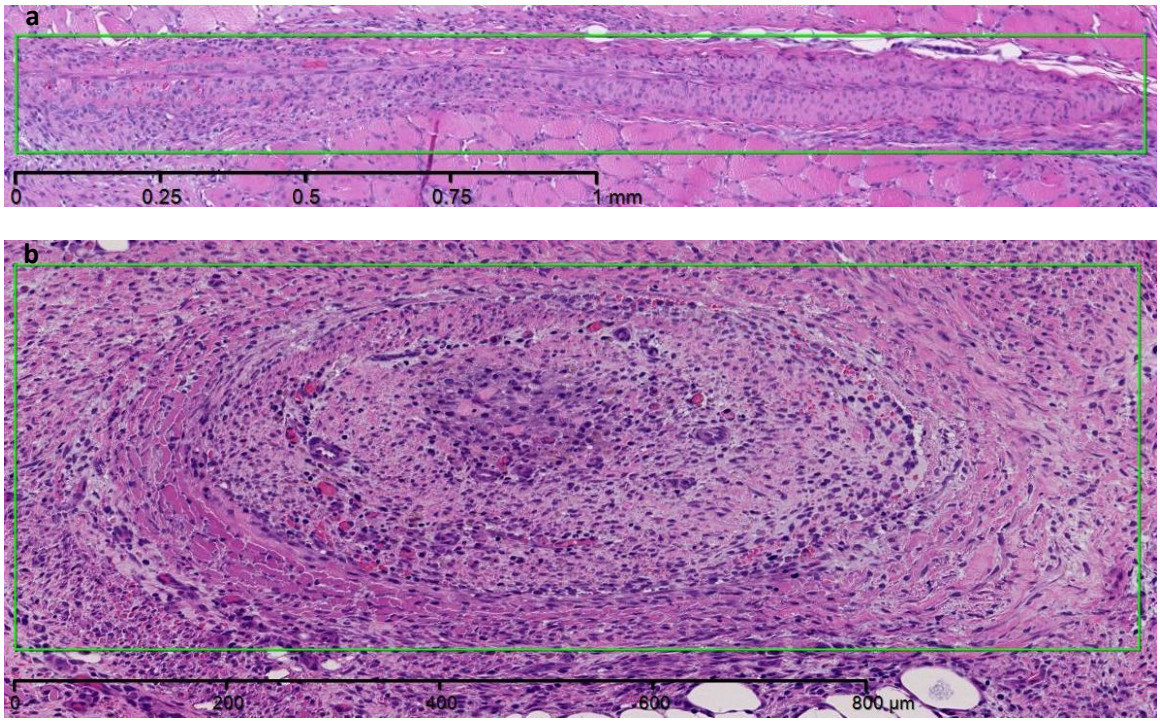

Figure 9: HE sections (magnification 5×) of representative saphenous veins (green rectangles) showing a transmural thickening and collapse of their lumens. The sections (a) and (b) respectively correspond to veins treated according to protocols (2) and (3).

The lesions observed on samples sonicated with moving pulses were histologically identical to those treated with fixed pulses. However, variability in the severity of the lesions was observed between samples. The majority (73%) of samples treated with fixed pulses showed a severe thrombo-vasculitis while lesions were evenly distributed between severe and moderate for samples sonicated with moving pulses.

Discussion

The feasibility of inducing sustainable vascular occlusion with HIFU thermal effects was demonstrated since histology reported 82% of vascular occlusion. Occlusion was successful in all cases where compression was applied.

Histological analysis systematically showed severe lesions for samples which underwent fixed point-by-point sonications and moderate lesions for half of the ones that were treated

by moving pulses. With moving pulses, the energy delivered is more spread and results in less severe lesions.

However, vein samples that showed no occlusion were treated with fixed pulses. According to simulations in the orthogonal direction to the vein diameter, coagulated zone after fixed pulses is barely enough to cover the vein. Fixed pulses are effective when the vein wall is completely encompassed in the lesion.

After fixed pulses, the coagulated zone is 2.4 mm in diameter and does not cover the whole circumference of all targeted veins (diameter range between [1.1 – 3.7 mm].

Conversely, moving pulses cover an area 1.8 times wider which reliably damage the whole circumference of all the veins. However, treatment with moving pulses required nearly three times more sonications than treatment with fixed pulses to treat a same vein segment.

The lack of symmetry observed in the figure 5 resulted from heat accumulation effect. As sonications are delivered, thermal energy deposited by previous pulse is added to energy deposition of current pulse. There is therefore an overlap in heat accumulation between successive pulses.

Although temperature dependence of ultrasound parameters has been demonstrated experimentally [38,39,48,49,40–47], constant acoustic parameters were used in the simulation as done by other teams[50–53]

In this study, we did not investigate focus movement speeds higher than 0.75 $mm.s^{-1}$ but further work may be performed to assess the highest focus speed that can lead to both a fast and an effective occlusion.

Considering the good correlation between simulations and histologic findings, the model used to assess thermal damage in the vein, based on the denaturation of collagen, appears to be consistent. This is supported by the study conducted by Fujiwara et al [54] where vessel occlusion was observed when peak temperature of the insonated sample hit 98°C but not at 47°C or 54°C.

Area corresponding to denaturation of 99% of native proteins correlates with the region where temperature reached 85°C. This temperature is also the level recommended by radiofrequency closure ablation to seal veins.

By heating homogeneously the intima to 85°C, we would mostly likely achieve total coagulation of the vein wall.

In our study, the three occlusion-free samples correspond to treatments without compression. We hypothesize that blood flow could have acted as a heat sink which prevented the temperature elevation of the vein wall from reaching sufficient levels. Compression should be considered for future clinical treatments as it helps to abolish blood flow and to decrease lumen area.

The high temperature elevations obtained in the simulations indicate that in our study, thermal effects of HIFU are expected to play a major role in our venous occlusions. Thermal mechanism compares favorably to the use of purely mechanical occlusion effects as reported by Hwang et al [55], which lead to a recanalization of the veins after the treatment. Hwang et al [55] used pulsed HIFU exposures with a low duty cycle in synergy with ultrasound contrast agent. The treatment was effective but could not maintain rabbit auricular vein occlusion over 14 days. With similar pulsing regime (9 MPa peak rarefaction pressure, 1-Hz pulse repetition frequency), Zhou et al [15] demonstrated a sustainable occlusion with mechanical effects of HIFU but only by injecting pro-inflammatory agents corresponding to the detergents found in sclerosing agents [56].

Groups who used ultrasound alone reported a temporary occlusion that did not exceed one week after treatments [8,54,57]. Notwithstanding that they have demonstrated occlusion in small veins (<1.5 mm), no long-term occlusion was proved.

Our exposure ultrasound parameters without additives were sufficient to induce venous closure. To date and to the best of our knowledge, no other study reported noninvasive permanent occlusion on veins of similar size, with the use of thermal effects of HIFU.

Conclusion

In this study, two sonication strategies have been identified and evaluated in a rabbit model. *In vivo* experiments have demonstrated that thermal ablation with HIFU can induce permanent sealing of veins of up to 3.7 mm [1.1-3.7 mm] in diameter.
HIFU is thereby a promising alternative to treat incompetent perforating veins. The treatment parameters used in this study provide insights for subsequent clinical trials.
Vein compression was identified as a key factor contributing to successful vascular occlusion since it avoided the cooling effect of the blood flow.

Future work should demonstrate the ability to coagulate larger veins (in a larger animal model) similar to the great saphenous vein and its tributaries.

References

[1] Alam M, Nguyen T H and Dover J S 2006 *Treatment of Leg Veins* (Elsevier)

[2] Goldman MP 2000 Closure of the great saphenous vein with endoluminal radiofrequency thermal heating in combination with ambulatory phlebectomy: preliminary 6-month follow-up *Dermatol Surg* **26** 452–6

[3] Navarro L, Min R J and Bone C 2001 Endovenous laser: a new minimally invasive method of treatment for varicose veins-preliminary observations using an 810 nm diode laser *Dermatol Surg* **27** 117–22

[4] Manfrini S, Gasbarro V, Danielsson G, Norgren L, Chandler J G, Lennox A F, Zarka Z a. and Nicolaides A N 2000 Endovenous management of saphenous vein reflux *J. Vasc. Surg.* **32** 330–42

[5] Bergan J, Kumins N, Owens E and Sparks S 2002 Surgical end endovascular treatment of lower extremity venous insufficieency *J. Vasc. Interv. Radiol.* **13** 563–8

[6] Dillavou E D, Harlander-Locke M, Labropoulos N, Elias S and Ozsvath K J 2016 Current state of the treatment of perforating veins *J. Vasc. Surg.* **4** 131–5

[7] Delon-Martin C, Vogt C, Chignier E, Guers C, Chapelon J Y and Cathignol D 1995

Venous thrombosis generation by means of high-intensity focused ultrasound *Ultrasound Med. Biol* **21** 113–9

[8] Hynynen K, Chung A H, Colucci V and Jolesz F A 1996 Potential adverse effects of high-intensity focused ultrasound exposure on blood vessels in vivo *Ultrasound Med. Biol* **22** 193–201

[9] Hynynen K ;, V C, Chung A and Jolesz F 1996 Noninvasive arterial occlusion using MRI-guided focused ultrasound *Ultrasound Med. Biol* **22** 1071–7

[10] Rivens I H, Rowland I J, Denbow M, Fisk N M, Ter Haar G R and Leach M O 1999 Vascular occlusion using focused ultrasound surgery for use in fetal medicine *Eur. J. Ultrasound* **9** 89–97

[11] Denbow M L, Rivens I H, Rowland I J, Leach M O, Fisk N M and ter Haar G R 2000 Preclinical development of noninvasive vascular occlusion with focused ultrasonic surgery for fetal therapy *J Obs. Gyneco* 387–92

[12] Ishikawa T, Okai T, Sasaki K, Umemura S ichiro, Fujiwara R, Kushima M, Ichihara M and Ichizuka K 2003 Functional and histological changes in rat femoral arteries by HIFU exposure *Ultrasound Med. Biol.* **29** 1471–7

[13] Fujiwara K, Takeuchi H, Itani K, Yoshinaka K, Sasaki A, Azuma T, Sakuma I, Matsumoto Y, Medical H A, High T, Focused I and Aloka H 2011 Real time HIFU beam imaging *Proc. 2001 Symp. Ultrason. Electron.* **32** 583–4

[14] Hwang J H, Tu J, Brayman A A, Matula T J and Crum L A 2006 Correlation between inertial cavitation dose and endothelial cell damage in vivo *Ultrasound Med. Biol* **32** 1611–9

[15] Zhou Y, Zia J, Warren C, Starr F L, Brayman A A, Crum L A and Hwang J H 2011 Targeted long-term venous occlusion using pulsed high-intensity focused ultrasound combined with a pro-inflammatory agent *Ultrasound Med Biol* **37** 1653–8

[16] Hwang J H, Brayman A A, Reidy M A, Matula T J, Kimmey M B and Crum L A 2005 Vascular effects induced by combined 1-MHz ultrasound and microbubble contrast agent treatments in vivo *Ultrasound Med. Biol* **31** 553–64

[17] Hwang J H, Zhou Y, Warren C, Brayman A A and Crum L A 2010 Targeted venous occlusion using pulsed high-intensity focused ultrasound. *IEEE Trans. Biomed. Eng.* **57** 37–40

[18] Ichizuka K, Ando S, Ichihara M, Ishikawa T, Uchiyama N, Sasaki K, Umemura S, Matsuoka R, Sekizawa a, Okai T, Akabane T and Kushima M 2007 Application of high-intensity focused ultrasound for umbilical artery occlusion in a rabbit model. *Ultrasound Obstet. Gynecol.* **30** 47–51

[19] Ichiharan Mitsuyoshi, Sasaki K, Umemura S-I, Kushima M and Okai T 2007 Blood flow occlusion via ultrasound image-guided high-intensity focused ultrasound and its effect on tissue perfusion *Ultrasound Med. Biol* **33** 452–9

[20] Shaw C J, ter Haar G R, Rivens I H, Giussani D A and Lees C C 2014 Pathophysiological mechanisms of high-intensity focused ultrasound-mediated vascular occlusion and relevance to non-invasive fetal surgery *J. R. Soc. Interface* **11**

[21] Zhang M, Fabiilli M L, Haworth K J, Fowlkes J B, Kripfgans O D, Roberts W W, Ives K A and Carson P . 2010 In vivo investigation of acoustic droplet vaporization for occlusion in canine kidney *Ultrasound* **36** 1691–703

[22] Kovatcheva R, Guglielmina J-N, Abehsera M, Boulanger L, Laurent N and Poncelet E 2015 Ultrasound-guided high-intensity focused ultrasound treatment of breast fibroadenoma-a multicenter experience *J. Ther. Ultrasound* **3** 1

[23] Esnault O, Franc B, Leenhardt L, Rouxel A, Ménégaux F and Lacoste F 2006 High-Intensity Focused Ultrasound (Hifu) Treatment For Thyroid Nodules: Experimental and First Clinical Studies *6th International Symposium on Therapeutic Ultrasound* vol 911 (AIP) pp 98–103

[24] Treeby B E and Cox B T 2010 k-Wave: MATLAB toolbox for the simulation and reconstruction of photoacoustic wave fields *J. Biomed. Opt.* **15** 021314-1: 021314-12

[25] Grisey A, Yon S, Letort V and Lafitte P 2016 Simulation of high-intensity focused ultrasound lesions in presence of boiling *J. Ther. Ultrasound* **4** 11

[26] Grisey A, Heidmann M, Letort V, Lafitte P and Yon S 2016 Influence of Skin and

460 Subcutaneous Tissue on High-Intensity Focused Ultrasound Beam: Experimental
461 Quantification and Numerical Modeling *Ultrasound Med. Biol* **42** 2457–65
462 [27] Duck F A 1990 Acoustic Properties of Tissue at Ultrasonic Frequencies *Phys. Prop.*
463 *Tissues* 73–135
464 [28] Pennes H H 1948 Analysis of tissue and arterial blood temperatures in the resting
465 human forearm. *J. Appl. Physiol.* **1** 93–122
466 [29] Kozma C, Macklin W, Cummins L M and Mauer R 1974 *The Biology of the Laboratory*
467 *Rabbit* ed S H Weisbroth, R E Flatt and A L Kraus (United States of America:
468 Academic Press Inc. (London) Ltd.)
469 [30] Duck F A 1990 Thermal Properties of Tissue *Phys. Prop. Tissues* 9–42
470 [31] Agah R, Pearce J A, Welch A J and Motamedi M 1994 Rate process model for arterial
471 tissue thermal damage: Implications on vessel photocoagulation *Lasers Surg. Med.* **15**
472 176–84
473 [32] Pankhurst K 1947 Incipient Shrinkage of Collagen and Gelatin *Nature* **159** 538
474 [33] Chent L, Ter Haart G, Hill C R, Dworkint M, Carnochant P, Young H and Benstedt J P
475 M 1993 Physics in Medicine & Biology Effect of blood perfusion on the ablation of
476 liver parenchyma with high-intensity focused ultrasound *Phys. Med. Biol* **38** 1661–73
477 [34] Goldberg S N, Stein M C, Gazelle G S, Sheiman R G, Kruskal J B and Clouse M E
478 1999 Percutaneous Radiofrequency Tissue Ablation: Optimization of Pulsed-
479 Radiofrequency Technique to Increase Coagulation Necrosis *J. Vasc. Interv. Radiol.*
480 907–16
481 [35] Heisterkamp J, Hillegersberg R van, Mulder P G ., Sinofsky E L and Ijzermans J N .
482 1997 Importance of eliminating portal flow to produce large intrahepatic lesions with
483 interstitial laser coagulation *Br. J. Surg.* 1245–8
484 [36] Patterson E J, Scudamore C H, Eng E, Owen D A, Nagy A G and Buczkowski A K
485 1998 Radiofrequency Ablation of Porcine Liver In Vivo Effects of Blood Flow and
486 Treatment Time on Lesion Size *Ann. Surg.* **227** 559–65
487 [37] Dorr L N and Hynynen K 1992 The effects of tissue heterogeneities and large blood

vessels on the thermal exposure induced by short high-power ultrasound pulses *Int. J. Hyperth.* **8** 45–59

[38] Chato J . 1985 Measurement of thermal properties of biological materials *Heat Transf. Med. Biol.* **1** 167–92

[39] Valvano J W, Cochran J R and Diller K R 1985 Thermal Conductivity and Diffusivity of Biomaterials Measured with Self-Heated Thermistors *Int. J. Thermophys.* **6** 301–11

[40] Valvano J . and Chitsabesan B 1987 Thermal conductivity and diffusivity of arterial wall and atherosclerotic plaque *Lasers Life Sci.* **1** 219–29

[41] Gammell P M, Le Croissette D H and Heyser R C 1979 Temperature and frequency dependence of ultrasonic attenuation in selected tissues *Ultrasound Med. Biol* **5** 269–77

[42] Damianou C A, Sanghvi N T, Fry F J and Maass-Moreno R 1997 Dependence of ultrasonic attenuation and absorption in dog soft tissues on temperature and thermal dose *J. Acoust. Soc. Am.* **102** 628–34

[43] Gertner M R, Wilson B C and Sherar M D 1997 Ultrasound properties of liver tissue during heating *Ultrasound Med. Biol.* **23** 1395–403

[44] Techavipoo U, Varghese T, Zagzebski J A, Stiles T and Frank G 2002 Temperature Dependence of Ultrasonic Propagation Speed and Attenuation in Canine Tissue *Ultrason. Imaging* **24** 246–60

[45] Zderic V, Keshavarzi A, Andrew M A, Vaezy S and Martin R W 2004 Attenuation of porcine tissues in vivo after high-intensity ultrasound treatment *Ultrasound Med. Biol.* **30** 61–6

[46] Choi M J, Guntur S R, Lee J M, Paeng D G, Lee K I L and Coleman A 2011 Changes in ultrasonic properties of liver tissue in vitro during heating-cooling cycle concomitant with thermal coagulation *Ultrasound Med. Biol.* **37** 2000–12

[47] Ghoshal G, Luchies A C, Blue J P and Oelze M L 2011 Temperature dependent ultrasonic characterization of biological media *J. Acoust. Soc. Am.* **130** 2203–11

[48] Jackson E, Coussios C and Cleveland R 2014 Nonlinear acoustic properties of ex

vivo bovine liver and the effects of temperature and denaturation *Phys. Med. Biol* **59** 3223

[49] Bamber, J.C Hill C . 1979 Ultrasonic attenuation and propagation sped in mammalian tissues as a function of temperature *Ultrasound Med. Biol.* **5** 149–57

[50] Constans C, Mateo P ., Tanter M and Aubry J . 2018 Potential impact of thermal effects during ultrasonic neurostimulation : retrospective numerical estimation of temperature elevation in seven rodent setups *Phys. Med. Biol.* **63**

[51] Eikelder H H ten;, Bosnacki D D, Elevelt A, Donato K, Tullio A D, Breuer B B, Wijk J van;, Dijk E E van;, Modena D, Yeo S S Y and Grüll H H 2016 Modelling the temperature evolution of bone under high intensity focused ultrasound *Phys. Med. Biol.* **61**

[52] Pinton G, Aubry J-F, Fink M and Tanter M 2011 Effects of nonlinear ultrasound propagation on high intensity brain therapy *Med. Phys.* **38** 1207–16

[53] Meaney P M, Clarke R L, Ter Haar G R and Rivens I H 1998 A 3-D finite-element model for computation of temperature profiles and regions of thermal damage during focused ultrasound surgery exposures *Ultrasound Med. Biol.* **24** 1489–99

[54] Fujiwara R, Sasaki K, Ishikawa T, Suzuki M, Umemura S-I, Kushima M and Okai T 2002 Arterial Blood Flow Occlusion by High Intensity Focused Ultrasound and Histologic Evaluation of Its Effect on Arteries and Surrounding Tissues *J Med Ultrason.* **29** 85–90

[55] Hwang J H, Zhou Y, Warren C, Brayman A A and Crum L A 2010 Targeted venous occlusion using pulsed high-intensity focused ultrasound *IEEE Trans Biomed Eng* **57** 37–40

[56] Loffroy R, Guiu B, Cercueil J-P and Krause D 2009 Endovascular Therapeutic Embolisation: An Overview of Occluding Agents and their Effects on Embolised Tissues *Curr. Vasc. Pharmacol.* **7** 250–63

[57] Hynynen K, Colucci V, Chung A and Jolesz F 1996 Noninvasive arterial occlusion using MRI-guided focused ultrasound *Ultrasound Med. Biol* **22** 1071–7

544